# Self-Ordering within Thin Films of Poly(olefin sulfone)s

**Richard W. Date,[†] Allan H. Fawcett,[*,†] Thomas Geue,[§] Jörn Haferkorn,[‡] R. Karl Malcolm,[†] and Joachim Stumpe[*,‡]**

*School of Chemistry, The Queen's University of Belfast, Belfast BT9 5AG, Northern Ireland, United Kingdom, U.K., Department of Chemistry, Humboldt University Berlin, Erieseering 42, D-10319 Berlin, Germany, and Department of Physics, University of Potsdam, Am Neuen Palais 10, D-14469 Potsdam, Germany*

*Received December 16, 1997; Revised Manuscript Received April 13, 1998*

ABSTRACT: A study has been performed of the manner in which two structural features of poly(olefin sulfone)s, helical backbones and calamitic side chains, create order in films. For this purpose copolymers were prepared with one (polymer **I**) or two (polymer **III**) cyanobiphenyls per residue, and terpolymers were prepared with both such residues diluted to below the 5% level within an otherwise poly(eicosene sulfone) chain (respectively, polymers **II** and **IV**). The polymers all have ordered phases according to X-ray powder diffraction studies on samples cooled from the melt, a layer spacing of about 45 Å being detected in the films as in the bulk. Those polymers with mainly eicosene sulfone residues had crystalline phases with large domains, the layers deriving from the helical backbones alone, the smectic A phases of the parent poly(eicosene sulfone) being either suppressed or reduced in extent by the presence of the aromatic moieties, which were almost randomly orientated. Those with one or two cyanobiphenyls per residue were liquid crystalline. In the latter the layer spacing derives from both backbone and side chains and is reduced when the residues bear a second mesogen as a consequence of a constraining effect from the stiff backbone, as a novel model predicts. The spacers give rise to a glass transition and segregate the planes in which the stiff backbones are assembled from the regions in which the aromatic groups aggregate on account of the strong $\pi-\pi^*$ interactions. Amorphous and optically isotropic spun cast films of these polymers became ordered on cooling from the melt or just on annealing, with the order, as determined by studies on the optical properties, being homeotropic for the aromatics and being planar for the backbones in a monodomain. For this arrangement we introduce the term homeo-planar smectic. Order parameters as high as 0.63 were measured for polymer **I**, from a clear film. The cyanobiphenyl chromophores formed H aggregates, with blue shifts in absorption and red shifts in fluoresence, and a little surprisingly these resulted in a circular dichroism, detectable when the films were inspected at an angle of 45° to the normal.

## Introduction

In this investigation we report the self-ordering properties of thin films of several poly(olefin sulfone)s, polymers that are readily prepared by the free radical polymerization of alkenes and sulfur dioxide and have an alternating structure $-(CH_2-CHR-SO_2)_n-$.[1] Liquid crystallinity has been found not only in those polysulfones that bear a conventional calamitic mesogenic group in the side chain[2−5] but also in those with merely a long paraffinic side chain.[6,7] In the latter case the ordering structure is the backbone itself, which despite being atactic as made by the free radical copolymerization of $SO_2$ with an olefin[8,9] adopts a helical configuration. Strong electrostatic interaction between each pair of sulfone dipoles[8,10−12] locks the intervening three backbone bonds into a rather stable configuration. The regular orientation of the $-CH_2-CHR-$ sequences of the olefin residues then repeats this configuration, and creates the helical sections, each of which is terminated by kinks. The first evidence for this came from measurements of the dipole moments[8,10,13] in solution and has been supported by the observation with the electron microscope[14] of replica helices within isolated chains that had been dispersed upon a surface. Simple theories of these third-order Markov orientational correlations[8] and of chain dynamics[13,15] have been supplemented by force field calculations.[11] The ordering effect of the dipoles, as measured by the magnitude of the low-frequency relaxing dipole moment,[8] was found to be of less importance in dioxane,[16] whose polarity reduces the electrostatic ordering. Raising the temperature[16] similarly introduces more kinks and so reduces the dipole moment component created by the order within the one-dimensional array of dipoles on the polymer backbone in solution.

A second factor that stabilizes the helical configuration in solution of the backbone of the 1-olefin polysulfones is enhancing the length of the side chain. The order is present in polymers with ethyl side chains but is much greater if the side chain is lengthened to $C_{18}$.[11,17,18] The stiffness in such poly(eicosene sulfone) chains is reflected in the dipole moment of the isolated chains in solution, which reaches a limiting value of $\langle\mu^2\rangle/z$ only when $z$ reaches 1000.[12,13] According to the kinked helix model of the backbone conformations, the number of kinks located where backbone C−C bonds are in the trans conformation is reduced, and the mean length of the helical sections is correspondingly increased, by a mean field repulsion between the side chains of adjacent residues.[11] The polymers might best be described as kinked hairy rods, the presence of the kinks[8,11] distinguishing the polysulfones from the rigid rod types of hairy polymers based upon protein α-helices.[19,20] Kinks inserted chemically into the backbone have created a nematic texture in otherwise smectic

* Authors for correspondence.
† The Queen's University of Belfast.
‡ Humboldt University Berlin.
§ University of Potsdam.

S0024-9297(97)01827-5 CCC: $15.00 
Published on Web 07/10/1998

structure[7] by disrupting layers of backbones. The backbones of the polysulfones thus provide a self-ordering system in the bulk where one chain may influence its neighbors in one or two extra dimensions, which is interesting in its own right, but the behavior becomes more interesting when the side chains bear mesogenic structures. In this situation the two ordering components, backbone and side chain, may cooperate or frustrate each other in creating supramolecular layered structures, when no or little solvent is present.[7,21] Such questions are directed to the heart of understanding the nature of liquid crystallinity within bulk polymers.[22]

Anisotropic macroscopically ordered films of functionalized polymers are desirable for technical applications, so different methods for their preparation are currently being investigated.[23] The preparation of ordered films is complicated and time-consuming by the Langmuir−Blodgett technique, by building up layers one at a time chemically[24] or by nanofabrication of multicomposite films by adsorption from solution.[25] It is also difficult to achieve the alignment of LCP films by thermotropic self-organization on anisotropic surfaces or the use of AC electric fields.[26−28] Optically transparent, but isotropic, films of amorphous or liquid crystalline polymers can be prepared by spin-coating or casting. However annealing of LCP films usually results in polydomain structures which scatter light.[28]

Recently a smectic phase was established with a polysiloxane by spontaneous molecular self-assembly of the side chains starting from spin-coated films. Well-aligned homeotropic films of ferroelectric side and main chain polymers[29,30] were thus prepared. The formation of ordered structures via the interplay of liquid crystallinity and phase separation was shown for some block copolymers.[31] The surface segregation behavior caused a spontaneous ordering of lamellae on planar surfaces and the simultaneous ordering of LC domains. Phase separation in the vicinity of an air or substrate interface seemed to be different compared to the behavior in the bulk.

The creation of orientational and positional order within polymers may require aromatic moieties[32,33] the orientation of which may be measured using plane polarized light.[34] Between the chromophores there may be $\pi-\pi$ interactions causing apolar association or $\pi-\pi$ stacking. Within such van der Waals aggregates the transition moments of pairs of chromophores are coupled, and depending on their relative orientation, either H or J aggregates are established. The H aggregation of parallel orientation is recognized by a hypsochromic shift of absorbance and a bathochromic shift of fluorescence. The formation of such aggregates is stimulated by the supramolecular order in LB multilayers,[34−37] within liquid crystalline polymers[38−40] and in phase-separated liquid crystalline guest−host systems.[41] The development and presence of positional ordering may be monitored using X-rays, backbone order being recognized as the sulfur atoms are electron-rich. It will be interesting whether aggregates give rise to a measurable circular dichroism, as has been found for bilayers of achiral chromophores within micelles.[37,42]

In the present work we have synthesized a small number of poly(olefin sulfone)s containing the cyanobiphenyl mesogenic as shown in Scheme 1, so that we can systematically explore their ability to self-organize in thin spun-cast films. First in polymer **I**, the cyanobiphenyl mesogen has been placed on all residues. In polymer **II** the cyanobiphenyl mesogen is present only in a dilute, random fraction of residues within an otherwise poly(eicosene sulfone) chain so that the behavior of the isolated chromophore might be studied in an environment in which any order must derive from the backbones. In polymer **III** there are two cyanobiphenyl groups on each residue so side chain mesogenic effects are more important. Polymer **IV** has such

**Scheme 1. Polymer Structures**

Polymer I

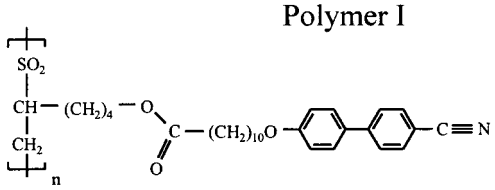

Polymer II

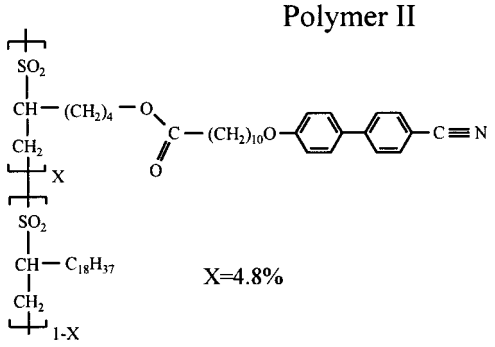


Polymer III

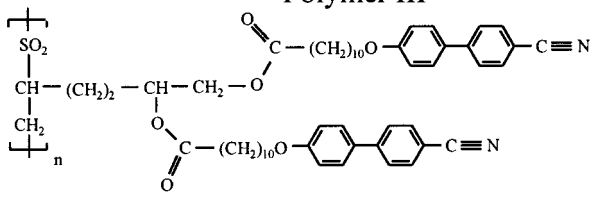

Polymer IV

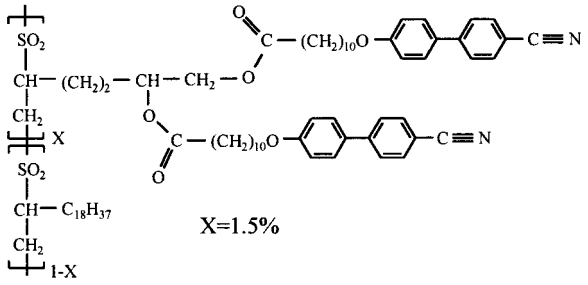


Polymer V

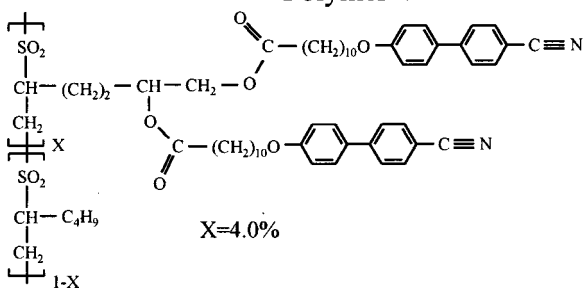


Polymer VI

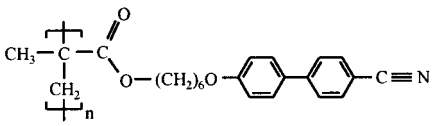

residues highly diluted within a environment of poly(eicosene sulfone) so that isolated pairs of cyanobiphenyl units can be examined. For comparison with these liquid crystalline systems, polymer **V** has a small fraction of cyanobiphenyl residues dispersed randomly in an amorphous poly(hexene sulfone) matrix.[7] The final polymer, **VI**, is a liquid crystalline cyanobiphenyl homopolymer with a methacrylate backbone obtained so that we might identify differences in the ordering properties of the polymers with the sulfone backbone.

The aim of this study is to investigate the interplay of ordering process of the poly(olefin sulfone) with a polar helical backbone of known pitch and the molecular aggregation of calamitic aromatic side groups in thin films, the intention being to attempt molecular engineering[43] on the nanometer scale[7] by varying the proportion of these features.

## Experimental Section

**Monomer Synthesis and Characterization. Synthesis of Hex-5-enyl 11-Bromoundecanoate.** 5-Hexen-1-ol (7.50 g, 74.9 mmol) and 11-bromoundecanoic acid (21.84 g, 82.4 mmol), *N*,*N*′-dicyclohexylcarbodiimide (16.95 g, 82.2 mmol), and dimethylaminopyridine (0.20 g, 1.60 mmol) were added to 100 mL of dry THF in a stoppered reaction flask and stirred for 72 h at room temperature. The dicyclohexylurea precipitate was filtered off and the filtrate columned on silica using chloroform as eluant to give a pale yellow liquid. Yield: 25.36 g, 97.5%.

**Synthesis of Hex-5-enyl 11-(4′-Oxy-4″-cyanobiphenyl)undecanoate, for monomer I.** Hex-5-enyl-11-bromoundecanoate (25.36 g, 73.0 mmol), 4-hydroxy-4′-cyanobiphenyl (14.95 g, 76.7 mmol), and anhydrous potassium carbonate (20.2 g, 146.0 mmol) were refluxed for 48 h in dry acetone. The inorganic residue was filtered off and the solvent removed from the filtrate, and the product was columned on silica using chloroform as eluant and then twice recrystallized from industrial alcohol and vacuum-dried. Yield: 25.85 g, 76.7%.

**Synthesis of Hex-5-enyl 1,2-Di(11-bromoundecanoate).** 11-Bromoundecanoic acid (25.2 g, 95.0 mmol) was added together with 20 mL of dry chloroform to a reaction flask flushed with dry nitrogen. Oxalyl chloride (13.26 g, 104.6 mmol) was added to 20 mL of dry chloroform and added dropwise to the reaction flask, and the reaction was stirred overnight at room temperature. The excess oxalyl chloride was removed and the reaction vessel flushed with dry nitrogen, hex-5-en-1,2-diol (5.00 g, 43.0 mmol) was dissolved in 20 mL of dry chloroform and added dropwise. After complete addition of the diol, the reaction was refluxed for 4 h. The product was columned on silica using chloroform as eluant. Yield: 22.60 g, 86.1%.

**Synthesis of Hex-5-enyl 1,2-di(11-(4′-oxy-4″-cyanobiphenyl)undecanoate), for Monomer III.** Hex-5-enyl 1,2-di(11-bromoundecanoate), (22.36 g, 36.62 mmol) 4-hydroxy-4′-cyanobiphenyl (15.00 g, 76.9 mmol), and anhydrous potassium carbonate (21.25 g, 153.1 mmol) were refluxed for 48 h in dry acetone. The inorganic residue was filtered off and the solvent removed from the filtrate. The product was columned on silica using chloroform as eluant and recrystallized twice from an industrial alcohol and ethyl acetate mixture and then vacuum-dried. Yield: 12.75 g, 41.5%.

**Polymer Synthesis and Characterization. Polymer I. Synthesis of Poly[hex-5-enyl 11-(4′-oxy-4″-cyanobiphenyl)undecanoate sulfone].** Hex-5-enyl 11-(4′-oxy-4″-cyanobiphenyl)undecanoate (3.00 g, 6.50 mmol) was dissolved in 30 mL of toluene and cooled in a cold bath maintained at −30 °C, and 4 mL of liquefied sulfur dioxide was added. *tert*-Butyl hydroperoxide (1.0 mL) was added dropwise at a rate of one drop approximately every 5 min. The reaction tube was left in the cold bath overnight and the polymer then precipitated from 200 mL of methanol, acidified with a few drops of concentrated hydrochloric acid, and filtered off. The polymer was then purified by dissolving in chloroform and reprecipitating twice more from methanol and then vacuum-dried. Yield 2.65 g, 78%.

**Polymer II. Synthesis of Poly[hex-5-enyl 11-(4′-oxy-4″-cyanobiphenyl)undecanoate sulfone]-*co*-poly[eicos-1-enesulfone].** The monomers hex-5-enyl-11-(4′-oxy-4″-cyanobiphenyl)undecanoate (0.292 g, 0.626 mmol) and eicos-1-ene (3.347 g, 11.93 mmol), corresponding to a 4.99% feed component for the biphenyl monomer, were dissolved in 50 mL of toluene and cooled in a cold bath maintained at −30 °C. Then, 4 mL of liquefied sulfur dioxide was added, and 1.0 mL *tert*-butyl hydroperoxide was added dropwise. The polymer was purified as for polymer **I**. Yield: 1.25 g, 28%. From $^1$H NMR we calculated that the polymer contained 4.8% of poly[hex-5-enyl-11 (4′-oxy-4″-cyanobiphenyl)undecanoate sulfone] residues.

**Polymer III. Synthesis of Poly[hex-5-enyl 1,2-di(11-(4′-oxy-4″-cyanobiphenyl)undecanoate) sulfone].** The monomer hex-1-ene-5,6-di(undecanoyl-4′-oxy-4″-cyanobiphenyl) (1.00 g, 1.19 mmol) was dissolved in 50 mL of chloroform and cooled in a cold bath maintained at −30 °C and, 4 mL of liquefied sulfur dioxide was added. The polymerization and purification was the same as used for polymer **I**. Yield: 0.50 g, 46%.

**Polymer IV. Synthesis of poly[hex-5-enyl 1,2-di(11-(4′-oxy-4″-cyanobiphenyl)undecanoate) sulfone]-*co*-poly[eicos-1-ene Sulfone].** The monomers hex-5-enyl 1,2-di(11-(4′-oxy-4″-cyanobiphenyl)undecanoate) (0.520 g, 0.626 mmol) and eicos-1-ene (3.347 g, 11.93 mmol), corresponding to a 4.99% feed component for the biphenyl monomer, were dissolved in 50 mL of toluene and cooled to in a cold bath maintained at −30 °C. Then 4 mL of liquefied sulfur dioxide was added, and 1.0 mL *tert*-butyl hydroperoxide was added dropwise. The polymer was purified as for polymer **I**. Yield: 2.05 g, 44%. From $^1$H NMR we calculated that the polymer contained 1.5% poly[hex-5-enyl 1,2-di(11-(4′-oxy-4″-cyanobiphenyl)undecanoate) sulfone] residues.

**Polymer V. Synthesis of poly[hex-5-enyl 1,2-di(11-(4′-oxy-4″-cyanobiphenyl)undecanoate) sulfone]-*co*-poly[hex-1-enesulfone].** The hex-5-enyl 1,2-di(11-(4′-oxy-4″-cyanobiphenyl)undecanoate) (1.049 g, 1.25 mmol) and hex-1-ene (2.00 g, 23.75 mmol), corresponding to a 5.00% feed component for the biphenyl monomer, were dissolved in 50 mL of toluene in a reaction tube and cooled in a cold bath maintained at −30 °C. Then 4 mL of liquefied sulfur dioxide was added, and 1.0 mL of *tert*-butyl hydroperoxide was added dropwise. The polymer was purified as for polymer **I**. Yield: 2.05 g, 44%. From $^1$H NMR we calculated that the polymer contained 4.0% of poly[hex-5-enyl 1,2-di(11-(4′-oxy-4″-cyanobiphenyl)undecanoate) sulfone] residues.

The results of molecular weight measurements recorded in Table 1 show that all are high polymers. They are above the range in which the clearing temperatures are molecular weight sensitive.[6] The DSC scans were

**Table 1. Molecular Weight[a] and Thermal Characteristics of the Polymers**

| polymer | $M_n \times 10^{-6}$ | $M_w/M_n$ | $T_g$/°C | $T_c$/°C | $\Delta H_c$/kJ mol$^{-1}$ | LC phases |
|---|---|---|---|---|---|---|
| **I** | 2.1 | 4.0 | 14 | 103 | 4.6 | $S_A$ |
| **II** | 1.8 | 2.9 | *b* | 49[c] | 20.4[c] | $S_B$,[c] $S_A$ |
| **III** | 5.4 | 2.0 | 17 | 149 | 6.7 | $S_A$ |
| **IV** | 0.67 | 5.3 | *b* | 50[c] | 21.3[c] | $S_B$[c] |
| **V** | 0.07 | 2.7 | 57[d] | | | $S_A$ |
| **VI** | 0.014 | 2.2 | 45 | 108[e] | *f* | $S_A$, N |

[a] By G. P. C. with poly(styrene) standards. [b] Not detected down to −50 °C. [c] X-ray diffraction studies indicate a hexatic or crystalline smectic phase.[20] [d] $T_g$ step was followed by peak at 69 °C with an enthalpy of transition of 8.4J g$^{-1}$. [e] $S_A$ − N transition at 100 °C. [f] Not measured.

obtained with a DSC 7 (Perkin-Elmer) using a heating rate of 20 °C/min.

Spun-cast films of the polymers were prepared using a CT60 (Suss Techniques S. A.) spin coating system. The films were spun from 10% solutions of chloroform, using a speed of 2000 rpm, for 45 s at 25 °C after an acceleration 2000 rpm/s. In this way films of 300−500 nm thickness were achieved. Changing these parameters to 4000 rpm, 4000 rpm/s, and 15 s, respectively, resulted in films of 250−300 nm thickness, the film thickness being measured with a DETAC system. Silica glass substrates were used for the optical and the X-ray measurements. Some X-ray reflection investigations used films on a silicon wafer. Films were annealed by heating at 0.5−1 °C/min up to 2 °C below the clearing temperature. All samples remained at least 30 min at this temperature, before they were cooled slowly at 1−2 °C/min.

UV−visible measurements were measured using Lambda 2 and Lambda 19 instruments (Perkin-Elmer). The optical anisotropy was examined by polarized spectroscopy. Polarized UV−visible spectra were recorded on the Lambda 19 instrument, equipped with a set of Glan-Tayler prism polarizers made of calcite (LOT) driven by a computer-controlled stepper in steps of 5°. The polar plots show the orientational distribution at a chosen wavelength.

The films were examined in different positions in relation to the measuring beam. In the normal position, NP, the film was perpendicular to the horizontal propagation direction, *x*, of the beam, in the twisted position, YP, it is set an angle of 45° to the *x* and *y* directions, *y* being in the horizontal plane, and in the leaning position, ZP, it is set at an angle of 45° to the *x* axis and the vertical *z* axis, and at 0° to the *y* axis. When the film position was other than normal we allowed for the extra path length using the law of Huygens−Fresnel

$$E(\alpha) = [\,E(0°)]\,[(1 - n_s^{-2})\sin^2\alpha]^{-0.5} \qquad (1)$$

in which $n_s$ is the refractive index of the film and α the tilt angle. For $\alpha = 45°$, $E(\alpha)/E(0°) = 1.134$. In this case the extinction of the substrate and the loss of reflectivity were neglected.

To characterize the alignment we introduce the ratio[44]

$$R = A_{an}/A_{iso} \qquad (2)$$

where $A_{an}$ is the absorbance of the anisotropic film after annealing and $A_{iso}$ is the absorbance of the film in the isotropic state at the same wavelength of maximum absorbance before annealing, as in Figure 4. We relate *R* to an order parameter $S_\theta$ by

$$S_\theta = 1 - R = 1 - 3\langle\sin^2\theta\rangle/2 \qquad (3)$$

where θ is the angle between the transition dipole of the cyanobiphenyl chromophore and the normal to the plane.

A second measure of the azimuthal order, *D*, was found from the UV/Visible spectra obtained in the ZP position, as in Figure 4. If φ is the angle of the direction of the polarizer to the horizontal, *y*, axis then

$$D = A_{min}/A_{max} \qquad (4)$$

where $A_{max}$ is the maximum of angle dependent absorbance in the wavelength plot for a particular transition band and $A_{min}$ is the minimum for that band as φ was varied.

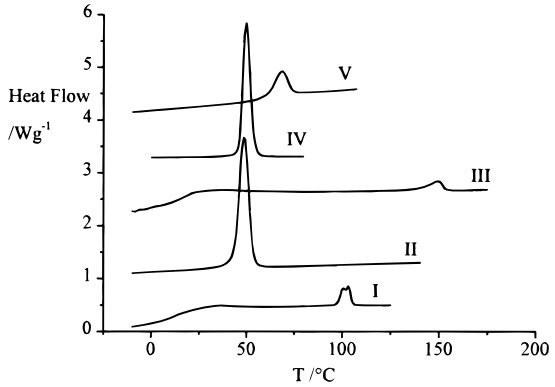


**Figure 1.** DSC traces for 10 to 15 mg samples of the following polymers recorded at 20 °C/min: polymer **I**, showing a glass transition and an endothermic transition, polymer **II**, showing an endothermic transition, polymer **III**, showing a glass transition and an endothermic transition, polymer **IV**, showing an endothermic transition, and polymer **V**, showing a modified glass transition feature.

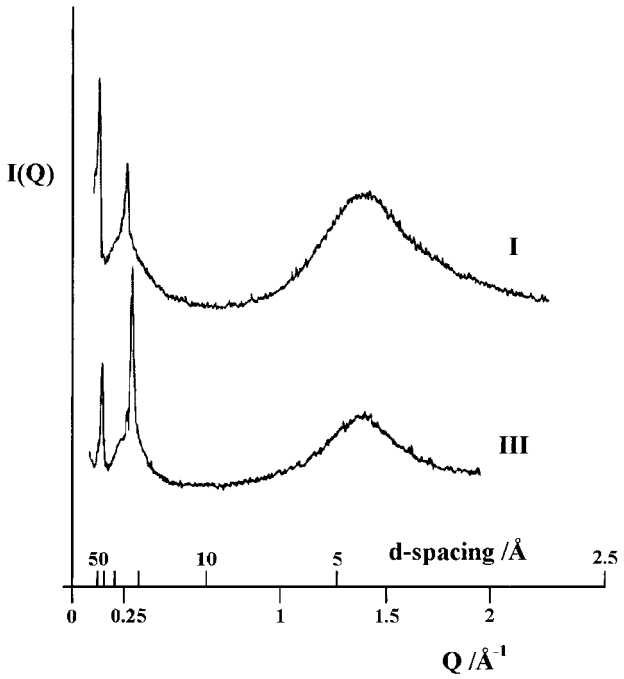


**Figure 2.** X-ray diffraction densitometer scans for bulk samples of polymer **I** at 70 °C and polymer **III** at 70 °C.

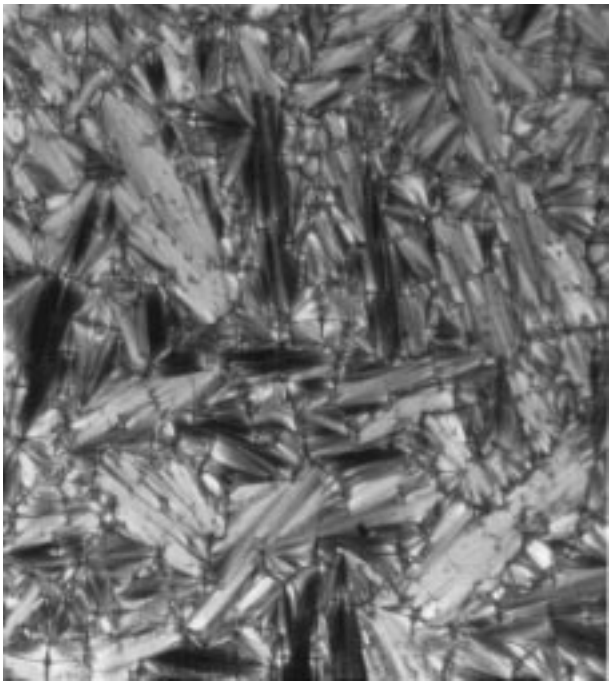

**Figure 3.** Focal conic texture of the smectic A phase of polymer **III** at 75 °C and ×80 magnification.

A spectroscopic order parameter, $S_p$, can be introduced, for measurements of the $\pi-\pi^*$ transition at a fixed wavelength, the wavelength being that at which the greatest absorbance was found as $\phi$ was rotated

$$S_p = (A_{max} - A_{min})/(A_{min} + A_{max}) \qquad (5)$$

Circular dichroism spectra were recorded with a JASCO 700. Fluorescence measurements were made using a LS 50 spectrometer (Perkin-Elmer). The films were excited at $\lambda = 300$ nm. The spectra were detected in a front face arrangement, with a 30° angle of the excitation beam with respect to the plane of the film. Optical microscopy studies on the polymers were made as previously reported.[6] Bulk X-ray diffraction patterns were recorded on sheets of photographic film using a Guinier diffraction camera fitted with a bent quartz monochromator (set to isolate Cu K$\alpha_1$ radiation $\lambda$ = 1.5405 Å). The films were scanned using a microdensitometer (Joyce-Loebl IIIc).

Measurements of X-ray reflectivity on thin films were made with an angle dispersive instrument, a $\theta-\theta$ diffractometer (STOE & Cie GmbH, Darmstadt, Germany), using a monochromatic beam, $\lambda$ = 1.54 Å, the angle of incidence and the detector angle being simultaneously monitored. However the resolution was not sufficient to detect structural changes during the scan or during heating.

The reflected intensity was then calculated based on the dynamical scattering theory by a Parrat formalism applying a kinematic model of Als-Nielsen.[45] In this the overall lamella is subdivided into several sublayers which all reflect the incoming monochromatic X-ray beam. The superposition of all reflected waves taking a phase shift into account gives the macroscopic observed reflection. The electron density profile in the $z$ direction along the surface normal is finally described by a box model.[45] Every layer is set to be a number of

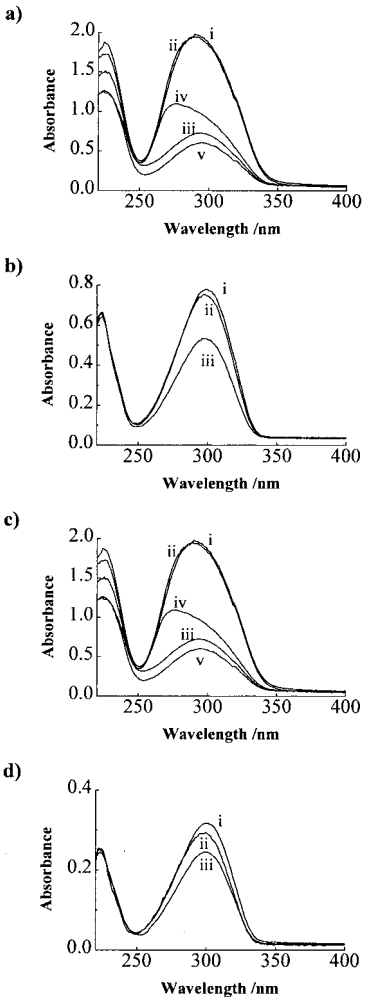


**Figure 4.** Absorbance of polymers **I** (a), **II** (b), **III** (c), and **IV** (d) as virgin (i) and annealed (iii) films in normal position NP and as virgin (ii) and annealed (iv) films in 45° leaning position ZP. In part a, the maximum and the minimum absorbance of the annealed film in ZP is monitored for parallel (iv) and perpendicular (v) positions of the polarizer.

sublayers characterized by sublamella thickness and a refractive index resulting in a smeared electron density profile. Stacked multilayers developed during annealing processes are calculated from several monolayer boxes. The measured electron density function is fitted via the introduction of an increasing number of layers with respect to interfacial and surface roughness.[46]

To obtain time-resolved measurements, we used an energy dispersive system.[47−49] The white spectrum of an X-ray tube strikes the sample at a fixed angle of incidence $\alpha_i$, and the reflected intensity is measured by a Si(Li) detector with a multichannel analyzer. The angle between detector and incident beam is $\theta = \alpha_i + \alpha_f$. An X-ray reflection spectrum shows Bragg peaks with a constant energy difference $\Delta E$ between two peaks of order $n$ and $n + 1$. $\Delta E$ [keV] is related to the layer distance $d$ [nm]:

$$d = \frac{hc}{\Delta E\ 2\ \sin(\theta/2)} \approx \frac{0.62}{\Delta E\ \sin\ \theta} \qquad (6)$$

For a quantitative evaluation the measured spectrum has to be corrected for the detector sensitivity and the energy dependent absorption of sample and air.

The grazing incidence diffraction measurements were carried out at beamline D4 and wiggler-beamline W1 at the Synchrotron Radiation Facility, Hasylab. A wavelength of $\lambda = 1.44$ Å was used in order to get best performance of the weak diffraction signals from the ultrathin polymer films. The intensity at beamline W1 was twice that compared for the Si/W multilayer at beamline D4, while the energy resolution increased by a factor of 30 ($\Delta E = 1$ eV) at $E = 8.611$ keV. The angle of incidence, $\alpha_i$, was usually set next to the critical angle, $\alpha_c = 0.17°$, and the beam was rectangularly focused (size 0.2 × 2 mm) on the samples placed on a vertically mounted heating platform. A position sensitive detector was used to simultaneously measure the angular position $\theta_{in}$ of the in-plane diffraction signals as well as the intensity distribution as a function of the exit angle $\alpha_f$ (rod scans). The resolution along $\alpha_f$ was 0.0055°. The collimation of the incoming monochromatic synchrotron beam was better than $\Delta\alpha_i \approx 0.005°$ and $\Delta\theta_{in} \approx 0.01°$. The (001) reflection was chosen for the measurements owing to the perpendicular arrangement of the net plane relative to the surface normal. The $2\theta_{in}$ angle was then fixed close to the measured in-plane Bragg position followed by a rotation around the surface normal ($\omega$-scan) to detect the appropriate angular position in $\omega$ which fulfilled the Bragg condition.[50]

The grazing incidence diffraction allows a depth resolution of the diffraction. If $L_i$ defines the length perpendicular to the surface for which the intensity is reduced by a factor of $e$, this can be expressed by[51]

$$L_i = (I_m q_z)^{-1} \tag{7}$$

Neglecting absorption of X-rays, $q_z$ is imaginary whenever $\alpha_i < \alpha_c$. In this case the incoming wave becomes evanescent, i.e., the exponentially damped wave propagates parallel to the sample surface. Their penetration depth of X-rays is very small, it amounts to about 44 Å for the investigations that took place below the critical angle. If $\alpha_i > \alpha_c$, $L_i$ is approximately defined by the linear photoabsorption coefficient, $\mu$, so $L_i \approx \sin \alpha_i/\mu$. For weakly absorbing materials, as in the present case, $L_i$ approaches 100 nm.

## Results and Discussion

The homopolymers with mesogenic side chains (**I** and **III**) have clearing temperatures of 103 and 149 °C (Table 1), values that are higher than that of poly(eicosene sulfone) at 68 °C[6] but much lower than that of a similar polymer with an α-helix within the backbone[52] (>250 °C). The increments are 35 °C for polymer **I**, with one cyanobiphenyl group, and 81 °C for polymer **III**, with two cyanobiphenyl groups, but the associated enthalpy changes are similar at about 4.6 kJ/mol, as shown in parts a and b of Figure 1. The ester groups in the side chains of the homopolymers, **I** and **III**, both have glass transitions at about 15 °C; see Figure 1. The steps in the specific heat capacity at the glass transition are 0.13 and 0.22 J deg$^{-1}$ mol$^{-1}$ for polymers **I** and **III**, respectively, reflecting the extra ester group in the spacer of the latter. For the terpolymers **II** and **IV**, which are predominantly poly(eicosene sulfone), below 0 °C the specific heat capacity is constant down to about −50 °C. The clearing temperatures at 50 °C are lower than that of poly(eicosene sulfone) itself, 68 °C,[6] a rather surprising depression when it is considered that there are just 0.03−0.05 cyanobiphenyl groups per residue.

**Table 2. UV/Visible Characteristics of Thin Films**[a]

| | effect of annealing | | | | | | polar scans | | | |
|---|---|---|---|---|---|---|---|---|---|---|
| | $\Delta\lambda_{max}$/nm | | | | | | $D$ in ZP | | $S_p$ in ZP | |
| polymer | NP | YP | ZP | $R$ | $S$ | $\theta$/deg | virg | ann | virg | ann |
| **I** | +6 | −17 | −15 | 0.37 | 0.63 | 29.8 | 0.97 | 0.56 | 0.02 | 0.42 |
| **II** | +1 | | −3 | 0.74 | 0.26 | 44.3 | 0.96 | 0.90 | 0.02 | 0.05 |
| **III** | +6 | −13 | −12 | 0.50 | 0.50 | 35.3 | 0.93 | 0.69 | 0.03 | 0.42 |
| **IV** | 0 | | −2 | 0.69 | 0.31 | 42.8 | 0.96 | 0.77 | 0.02 | 0.13 |
| **V** | 0 | | 0 | 1.00 | 0.00 | | 1.00 | 1.00 | 0.00 | 0.00 |
| **VI** | +2 | | +2 | 0.84 | 0.16 | 48.5 | 1.00 | 0.98 | 0.01 | 0.01 |

[a] $\Delta\lambda_{max}$ is the shift in absorbance maximum on annealing. NP is the normal position, YP is the twisted position, and ZP is the leaning position. $R$, $S$, $\langle\sin^2\theta\rangle$, $D$, and $S_p$ are terms describing the degree of alignment defined in equations 1−5. virg is the virgin film and ann is the annealed film.

The melting or clearing enthalpies are similar, but greater than that for poly(eicosene sulfone)[6] (8.2 kJ mol$^{-1}$), the aromatic groups are perhaps promoting a greater degree of crystallinity in the space between the backbones. The order within the paraffin side chains of these polymers these terpolymers is rather high, as the bulk X-ray diffraction studies show them to be hexatic or crystalline smectic phases.[21]

**X-ray Diffraction Measurements on Bulk Polymers.** Densitometer traces are shown in Figure 2 for polymers **I** and **III**, and the smectic layer spacings are given in Table 4. Following an inspection of the texture with the optical microscope, we made the following observations.

**Polymer I.** The X-ray diffraction pattern of the bulk polymer **I** at a temperature of 70 °C is shown in Figure 2. Two orders of sharp smectic layer diffraction peaks, corresponding to a layer spacing of 48.1 Å, were observed in the low-angle region, together with a diffuse peak in the wide-angle region corresponding to 4.8 Å. These characteristics identify the mesophase as a smectic A or C,[53] but from the optical microscopy studies in which we obtained some regions of homeotropic alignment, we can confirm it to be a smectic A phase. There also appeared to be a diffuse peak under the second-order layer diffraction peak at a spacing of about 26 Å which may come from an amorphous component.[54] The smectic layer spacing was measured to be 50 Å at 30 °C and was found to decrease gradually on heating to the clearing point at 103 °C, where it was 46.5 Å.

**Polymer II**. X-ray diffraction characterization of polymer **II** in the bulk showed it to form two mesophases, in contrast to the DSC observations, but the upper phase extended over only a few degrees. The higher temperature fluid smectic phase had a layer spacing of 41.5 Å. The diffuse peak in the wide-angle region corresponded to a spacing of 4.8 Å. The lower temperature phase was identified as a hexatic phase with a layer spacing of 42.0 Å, the diffraction peak in the wide-angle region being less diffuse. Similar behavior has been found for poly(eicosene sulfone) itself.[21]

**Polymer III.** The X-ray diffraction pattern of the mesophase polymer **III** at 70 °C, is shown in Figure 2, two orders of sharp smectic layer diffraction peaks, corresponding to a layer spacing of 44.1 Å, being observed in the low-angle region and a diffuse peak in the wide-angle region corresponding to 4.8 Å. These characteristics identified the mesophase as smectic A. There also appeared to be a diffuse peak under the second-order layer diffraction peak corresponding to a spacing of about 24 Å, which again may come from an amorphous component. The smectic layer spacing was

**Table 3. Fluorescence Characteristics of Thin Films[a]**

| | solution | | virgin film | | | annealed film | |
|---|---|---|---|---|---|---|---|
| polymer | $\lambda_{max}$/nm | fwhm/nm | $\lambda_{max}$/nm | fwhm/nm | $I_a/I_v$ | $\lambda_{max}$/nm | fwhm[a]/nm |
| **I** | 365 | 47 | 379 | 70 | 0.35 | 398 | 80 |
| **II** | 365 | 45.5 | 356 | 53 | 0.52 | 358 | 53.5 |
| **III** | 367 | 54 | 385 | 72 | 0.35 | 397 | 76 |
| **IV** | 364 | 47 | 356 | 65 | 0.68 | 357 | 70 |
| **V** | 367 | 54 | 367 | 53 | 0.99 | 367 | 53 |

[a] Key: fwhm, full width at half-maximum; $I_a/I_v$, intensity ratio of annealed to virgin film.

**Table 4. Smectic Layer and Other Spacing Measurements by X-ray Diffraction**

| | bulk *d*/Å | | | thin film[a] *d* /Å ± 1 | | |
|---|---|---|---|---|---|---|
| polymer | | | | | | |
| **I** | 50.0 (30 °C) | 48.1 (70 °C) | 46.5 (80 °C) | 47.6 | | |
| **II** | 43.1 ($S_B$, 30 °C) | | | 40.7 | 31.5 | 15.7 |
| **III** | 44.1 ($S_A$) (30 °C) | | | 41.9 | | |
| **IV** | 42.0 ($S_B$, 30 °C) | | 41.5 ($S_A$, 46 °C) | 40.0 | 20.0 | 15.9 |

[a] At ambient temperature ~25 °C.

**Scheme 2. Schematic Model of the Mesogenic Unit Packing within Polymer III[a]**

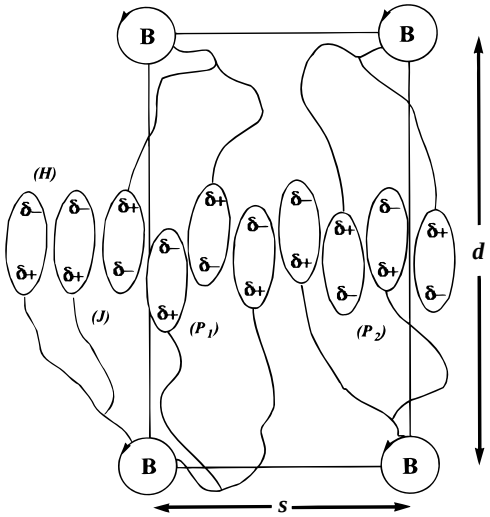


[a] B represents the helical backbones viewed along the helix axis, the pitch, *p*, being the distance above the page for a single turn. *d* represents the smectic layer and *s* the spacing between the backbones. (*H*) and *(J)* represent theoretical H and J aggregates respectively; ($P_1$) and ($P_2$) represent cyanobiphenyl groups with different degrees of overlap. The diagram shows an ideal alignment and orientation of one layer of backbones above another.

found to be 44.1 Å at 30 °C and to decrease gradually on heating to the clearing point at 149 °C where it was 41.8 Å.

**Polymer IV.** X-ray diffraction showed the copolymer to have a fluid smectic phase (smectic A or C), which had a layer spacing of 43.1 Å at 30 °C and of 41.5 Å at 62 °C.

We suggest a model of the polymers in Scheme 2 which has the helical sulfone backbones[6] arranged with a spacing, *d*, between the smectic layers of 40 to 50 Å separation. According to Mansfield[11] the pitch, *p*, is about 7 Å, there being 5 or 6 residues in a turn. As polymer **III** in optical studies can form a partly homeotropic texture, which is characteristic of a smectic A phase, the director for the cyanobiphenyls lies normal to the plane of the film. The focal conic texture observed by optical microscopy for polymer **III** is shown in Figure 3. The proposed structure for the mesophase is shown in Scheme 2 with partially overlapping cyanobiphenyl groups, in a partial bilayer smectic A phase ($S_{Ad}$),[55] and with the flexible spacers linked to each other before joining to the helices. The helices of one layer may not be parallel to those in its neighbors, though that is shown here. Within an ideal cuboid formed by the layer spacing, *d*, the distance *s* separating the helices within a layer, and the pitch, *p*, there are the cyanobiphenyl units of 5.5 residues. Taking the residue molecular weight of 903 for polymer **III** and assuming the density of a polysulfone[1] to be 1.00 g/cm$^3$, the volume of the cuboid is 8.24 × 10$^3$ Å$^3$. Taking a value of *d* as 44 Å and of *p* as 7.0 Å we calculate *s* to be 27 Å, which is close to the diffuse 24 Å spacing reported above in the X-ray pattern. If it comes from the intralayer spacing, the difference might readily be attributed to our assumed density being too low; some biphenyls[57] have a density of 1.4 g/cm$^3$. It would not be possible to reconcile these dimensions with a bilayer smectic A phase ($S_{A2}$) type of mesogen packing, so that the partial bilayer packing ($S_{Ad}$) shown in Scheme 2 is then supported. For polymer **I**, *d* is 50 Å, the residue molecular weight is 526, and *s* is found to be 14 Å (which is about half the 28 Å spacing noticed in the X-ray pattern). In this novel model the two controlling features are the Mansfield helix pitch[11] and the manner in which the mesogens pack, which is determined by their shape and dipole. If the cross-sectional area of the cyanobiphenyl group[56] is 20 Å$^2$, then for polymers **I** and **II** $p \times s$ should be respectively 110 and 220 Å$^2$ per residue. The volume of the disorganized spacers controls the remaining orthogonal distance, *d*, which is obtained by experiments. *d* is smaller for polymer **III** than for polymer **I** because the value of *s* for polymer **III** is twice that for polymer **I**. At low temperatures the spacer region vitrifies and causes the observed glass transition, which does have a higher step for **III** than for **I**. In monomeric 4-*n*-alkyloxy-4′-cyanobiphenyls, the weight of the all-trans conformation alkyl chain is higher in the liquid crystalline state than in the isotropic liquid,[57] but this may not be so for the spacers of these polymers, as their end-to-end distance is constrained by the need for them to pack within the region between the cyanobiphenyls and the backbones. The model does not predict whether there are H or J aggregates, or whether the degree of overlap corresponds to $P_1$ or to $P_2$.

**Optical Studies on the Films by UV−Visible Spectroscopy.** In chloroform all the polymers show very similar spectra, with the $\pi-\pi^*$ absorbance at 296 nm and the $\phi-\phi^*$ absorbance at 225 nm being caused

by the biphenyl moiety. Freshly prepared films were optically isotropic and showed the same shape of the spectra and wavelength of maximum absorbance ($\lambda_{max}$) as had those of the polymers in chloroform. The UV−visible spectra of the films spun on silica glass displayed large changes upon annealing the film at about 2 °C below the clearing temperature, followed by a slow cooling to room temperature. As may be seen in Figure 4 for the homopolymers **I** and **III**, the $\pi-\pi^*$ absorbances in the normal position fell to about 30% of the initial value, the fall being accompanied by a bathochromic shift of 6 nm. In contrast to the decrease of this band (characteristic for a transition of the aromatic moiety in the direction of the long axis of the chromophores), the $\phi-\phi^*$ absorbance band at 230 nm from transitions perpendicular to the long axis remained nearly constant, as in cases in which the rotation of the aromatic cores is not restricted. Terpolymers **II** and **IV**, containing only about 4.8 and 1.5%, respectively, of the cyanobiphenyl bearing residues amid a matrix of mainly poly(eicosene sulfone) residues, suffered no change in $\lambda_{max}$ and only a 25% fall in absorbance. A chemical reason for this decrease of absorbance may be excluded. The large fall of intensity indicated a significant out-of-plane orientation of the biphenyl chromophores, so we suspected a homeotropic alignment of the side groups upon annealing. To establish this effect for polymer **I**, an annealed film was examined with plane-polarized light, the sample being held in the laboratory frame with the film either normal to the beam (NP) or at an angle of 45° (YP or ZP) while the plane of polarization was rotated. The angle-dependent measurements show that the film is isotropic in the NP plane, but the annealing caused a significant decrease in absorbance. As the beam was rotated in the tilted positions YP and ZP, a significant anisotropy in absorbance is observed. Together with the change in $A_{max}$ there was a shift in $\lambda_{max}$ between 276 and 292 nm, as plots in Figure 4 indicate. Dichroism was largest at about 270 nm. The blue shift of the absorbance maximum, attributed to H aggregates, was found when the plane of the polarized light was vertical; the aggregates of the cyanobiphenyl units that form during the annealing are thus normal to the plane of the film. The absence of J aggregates from the spectra suggests that contact between mesogens attached to different layers may be of type $P_1$ (Scheme 2).

In the normal position (NP), both before and after annealing, polymer **I**'s absorbance was unaltered as the plane of polarization was rotated, showing that the chromophore was optically isotropic in the plane, as may be seen in parts a and b of Figure 5. However, when the annealed film was tilted vertically toward the measuring beam at an angle of 45° (ZP), near 300 nm the absorbance varied systematically with the angle of rotation of the planar polarized incident beam. This dichroism from the azimuthal absorbance of the chromophores may be seen in Figure 5. That the absorbance was a maximum when the plane of polarization was vertical and a minimum when the plane of polarization was horizontal confirms that the chromophores have become at least partially aligned. Both results can be caused by a homeotropic monodomain or by out of plane orientation of side groups in a polydomain structure. We investigated this further by inspecting areas about 10 $\mu$m across by optical microscopy.[58] It was found that successive annealings enhanced the extent of homeotropically aligned regions and extended a monodomain.

In Figure 6 we show how $S_P$ for polymer **I** is enhanced by one annealing and then stays fairly constant through five subsequent annealings. If the individual values of $A_{max}$ and $A_{min}$ are consulted, it may be seen that each becomes slightly smaller during each annealing, and that a limit may be approached. The nonpolarized measurements using eqs 2 and 3 as well as the polarized measurements using eqs 4 and 5 are summarized in Table 2. All LC poly(olefin sulfone)s show this ordering tendency, which is strongest for the two homopolymers **I** and **III**. So, in the annealed film of polymer **I** a homeotropic orientation with an order parameter $S_\theta = 0.63$ is established. The corresponding spectroscopic order parameter $S_p = 0.42$ was obtained from the homeotropically aligned film in the **ZP** arrangement of the sample.

The second homopolymer, polymer **III**, was made to enhance congestion within the aromatic side chains, and was similarly examined. In Figure 4c it is seen that annealing lowered the absorbance at 300 nm but made little difference to that at 225 nm. Studies after an overnight annealing found again that dichroism of the $\pi-\pi^*$ transition had developed, as the spectrum in Figure 4c and the polar scan of Figure 5h confirm. Further, we obtained the values for the parameters characterizing the optical order that are given in Table 2. By both factors S and D (ZP) polymer **I** is slightly more ordered than **III**, perhaps because the backbones are closer together in the backbone planes. Similar studies were also performed on the terpolymers **II** and **IV**, as shown in parts b and d, respectively, of Figure 4.

The importance of chromophore concentration for producing alignment and aggregation may be gauged from the measurements on the copolymers, polymers **II** and **IV**, in which the cyanobiphenyl groups are present in only 4.8% and 1.5%, respectively, of the side groups. After they were annealed, the spectra of these copolymers suffered a negligible change in wavelength and only a 25% fall of absorbance. For both polymers there was observed a bathochromic shift of only 2 nm in **ZP**, when the leaning position as $\phi$ was rotated (Figure 4b,d). The polar scans of Figure 5i indicate that there is only a little ordering of the cyanobiphenyl groups in the direction perpendicular to the plane of the film after annealing: in contrast to the homopolymers, a low anisotropy in the **ZP** position was established. A statistical distribution of the side groups did not allow sufficient aggregation to change $\lambda_{max}$ and the tendency for homeotropic orientation is smaller.

To clarify the role of the backbone structure in the annealing process we have examined a liquid crystalline poly(methacrylate), polymer **VI**, also bearing cyanobiphenyl moieties in the side group. The backbones are expected to have a random coil configuration.[59] In Figure 7 we present the UV−visible spectra of a film of polymer **VI**. It may be seen that the methacrylate polymer differs from polymer **I** (see Figure 4a), in that it has only a small decrease of absorption after annealing and no anisotropy, indicating that a layered structure and H aggregates are not formed. However, in contrast to the poly(olefin sulfones), annealing of the methacrylate polymer resulted in an increase of the background absorption caused by light scattering, indicating the formation of a polydomain structure.

Until now only liquid crystalline polymers have been considered. The amorphous polymer **V** has the same

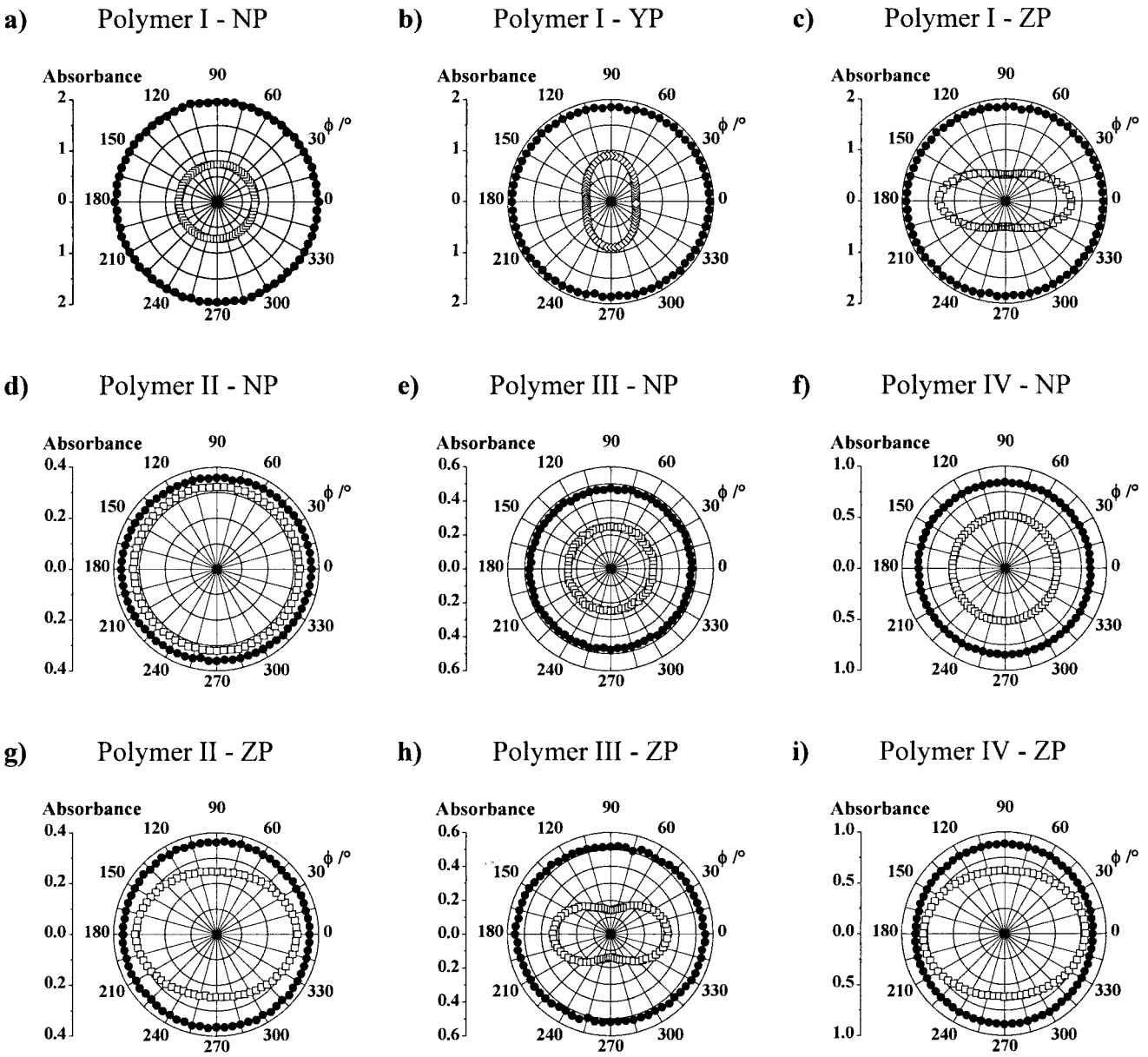


**Figure 5.** Angular-dependent absorbance for films of (a) polymer **I** in the normal position NP at 296 nm, (b) in the twisted position YP at 275 nm, and (c) in the leaning position ZP at 275 nm; (d) polymer **II** in NP at 298 nm and (e) polymer **III** in NP at 296 nm; (f) polymer **IV** in NP at 298 nm and (g) polymer **II** in ZP at 295 nm; and (h) polymer **III** in ZP at 275 nm and (i) polymer **IV** in ZP at 295 nm. (●) denotes virgin film measurements and (□) at same wavelength after annealing.

poly(olefin sulfone) backbone but does not show any change concerning absorbance, shift, and anisotropy on annealing for more than 10 h above the glass transition temperature at 57 °C for it does not have a liquid crystalline phase.[6] The liquid crystalline polymer **VI**, without a helical backbone, did not self-order upon annealing.

**Optical Studies of the Films by Fluorescence Spectroscopy.** We show fluorescence spectra of the liquid crystalline homopolymers **I** and **III**, the copolymer **IV**, and the amorphous copolymer **V** in Figure 8 in chloroform, and both before and after annealing spun films. For the films the excitation beam ($\lambda_{ex} = 300$ nm) was at 30° and the angle of detection at 60° to the normal, the paths being in the same plane. For the liquid crystalline homopolymers **I** and **III** the virgin films have $\lambda_{max}$ at 16 nm greater than in the solvent, but for the terpolymers **II** and **IV** $\lambda_{max}$ showed a bathochromic shift of about 8 nm in the film less than in the solvent (see Table 3). These are small medium effects. Stokes shifts of 56−100 nm were observed in the virgin films of the liquid crystalline polymers, the smallest, of 56 nm, being for copolymer **II** in which the cyanobiphenyl chromophores are isolated. Annealing of this film caused a minimal change of the shape of the fluorescence spectrum on the red-shift side, but there was not any change of the maximum fluorescence in front-face excitation. However the intensity was reduced by 65%. Within experimental error there was no change in the behavior of the film of the amorphous polymer **V** so all the changes in the other polymers are clearly linked to the processes of alignment and aggregation.

In the virgin films polymer **I** emitted at 379 nm, 5 nm below polymer **III**, but much above the terpolymers **II**, **IV**, and **V** in which the chromophores were dilute and isolated (Table 3). Annealing caused the emission of both of the liquid crystalline homopolymers to move

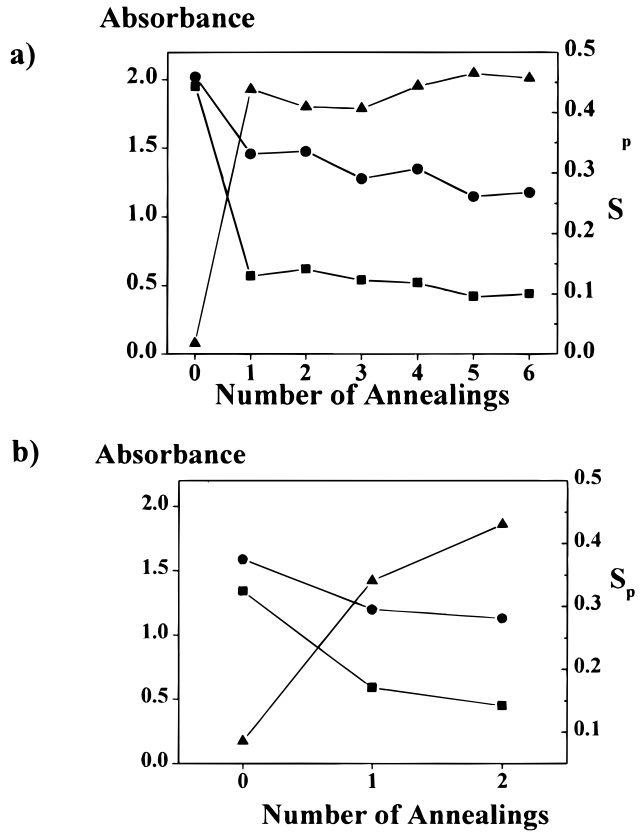


**Figure 6.** Maximum (○) and minimum (■) of absorbance and the spectroscopic degree of order (▲) in ZP versus the number of annealing processes for (a) polymer **I** and (b) polymer **III**.

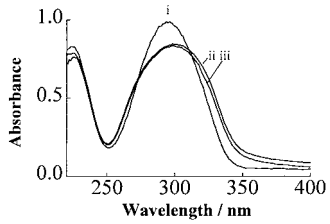


**Figure 7.** Absorbance of polymer **VI** as virgin film (i) and an annealed film (ii) in NP and as an annealed film (iii) in 45° leaning position ZP.

to 397 nm and caused the bandwidth to rise from 72 to 82 nm but did not influence the maxima of the other polymers: $\lambda_{max}$ remained at 356 nm for the liquid crystalline eicosenesulfone copolymers, **II** and **IV**, and at 367 nm for the hex-1-ene sulfone copolymer, **V**. There was also evidence for polymer **IV** for a shoulder at 400 nm that intensified a little on annealing, suggesting that the chromophores, found in pairs on the same residue, were then able to associate more after annealing in the parallel manner (H aggregates). This feature was absent from the spectrum of the terpolymers (**II** and **V**) which had a single chromophore diluted in the side chains, but was the main feature in the spectra of the well-endowed polymers **I** and **III**. We attribute the 400 nm feature in the fluorescence spectra of polymers **I** and **III** to an association of the chromophores. A further characteristic of annealing was that the intensity of the emitted light fell for the liquid crystalline polymers, to about 35% of that for the homopolymers **I** and **III**, and to about 52% of that for the terpolymers **II** and **IV**, but was unchanged when the amorphous terpolymer **V** was cooled from above its glass transition temperature.

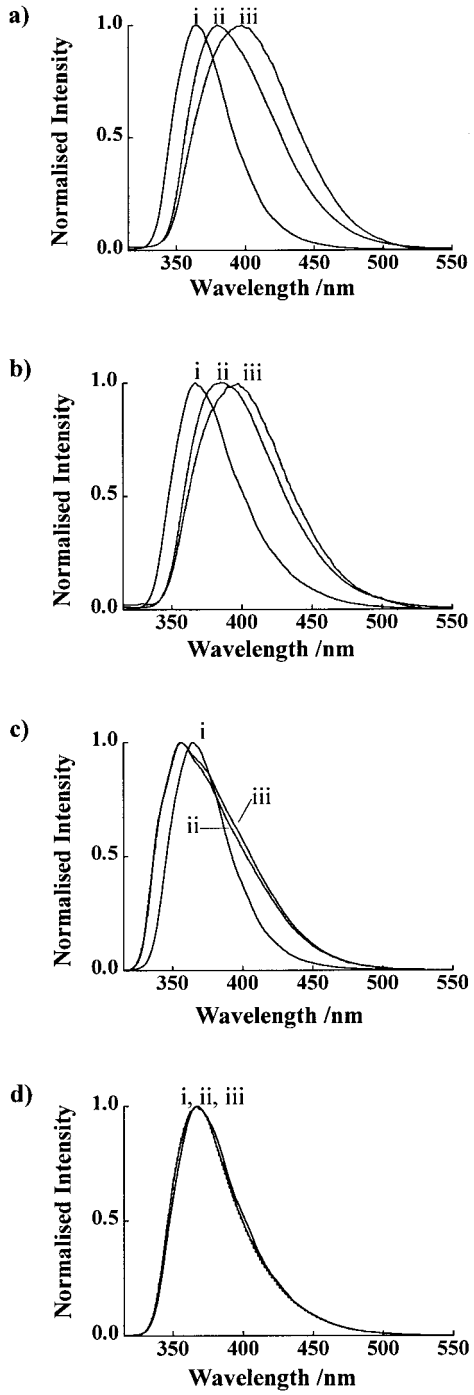


**Figure 8.** Fluorescence of the polymers **I** (a), **III** (b), **IV** (c), and **V** (d) in chloroform (i) and as virgin (ii) and annealed (iii) films.

Interactions of the chromophores in the ground and excited states may cause a bathochromic shift of fluorescence, the detected change is more probably caused by ground-state aggregation. It is well-known that H-aggregated species exhibit a weak fluorescence allowed by non-perfect order in the smectic A phase.

**X-ray Reflectivity Measurements and Grazing Incidence Diffraction of the Annealed Films.** We have monitored the development of a layered structure during the first annealing of an isotropically cast film of polymer I in an energy dispersive X-ray experiment. The sample was heated at 0.4 °C/min up to 86 °C and then held there for 60 min. The results are shown in Figure 9a. At 70 °C the system detected scattering in

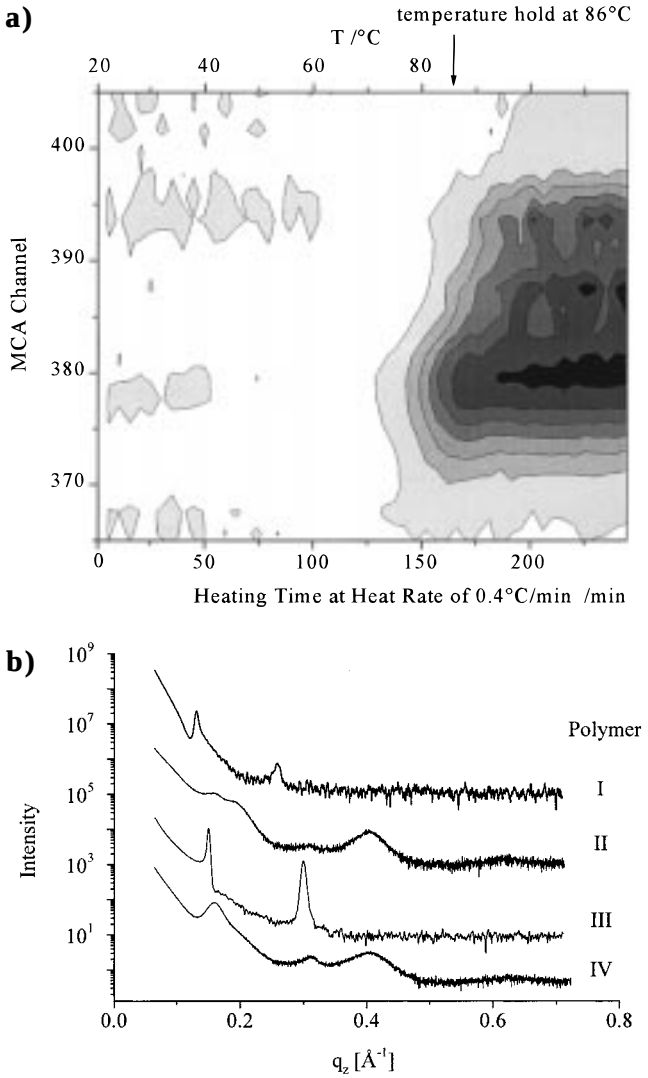


**Figure 9.** (a) Formation of the layered structure in spin coated film of polymer **I** with the development of first Bragg reflection, measured in an energy dispersive mode with less resolution but with sufficient signal to detect changes during a period of 1 min, at 17.168 keV (channel 380) on heating with 0.4 °C/min up to 86 °C. (b) SAXS Reflectivity curves of annealed films for **I**, **II**, **III** and **IV**.

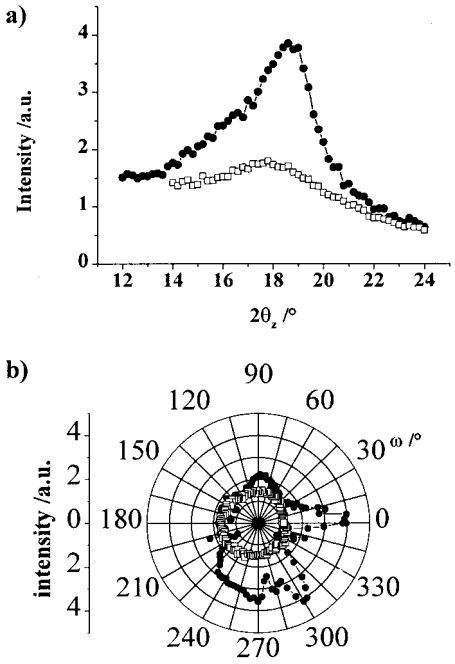


**Figure 10.** (a) 2:1 in-plane detector scans at grazing incidence for polymer **III** (□) with $\alpha_i = 0.14°$ and polymer **IV** (●) with $\alpha_i = 0.15°$ (IV) showing peaks at spacings of 4.4 and 4.5 Å respectively. (b) Corresponding scans around the surface normal at the angular position of the corresponding Bragg maxima.

channel 379, corresponding to ~48 Å, from the layer spacing, this signal increased quickly as the temperature rose and then more slowly once that was held. Thus film annealing, which produced an arrangement of side chain chromophores normal to the plane, was accompanied by the development of an extensive layer structure.

The scattering patterns obtained by means of SAXS from films of four of the polymers are shown in Figure 9b, where the two sharp peaks at room temperature may be seen for the homopolymers **I** and **III**. These layer spacings, *d*, are respectively, 47.6 and 41.9 Å and fall within the range found by the bulk powder diffraction measurements (Table 4). Calculation of the smectic layer correlation length from fitting of a calculated diffraction line shape to the experimental data[45,47] gives a value of 166 nm for the annealed polymer **I**. This is comparable with the thickness of the thin film and indicates a very well developed smectic layer structure. The diffuse diffraction feature observed at about 25 Å in the diffraction patterns of Figure 2 were not seen in Figure 9b, so annealing may have removed any amorphous content from these films.

The thin film of polymer **IV** has a broad SAXS peak corresponding to a spacing of 15.9 Å together with two orders of the smectic layer peaks corresponding to a spacing of 40 Å. These peaks are more diffuse than that of poly(eicosene sulfone)[21] as the guest residues disrupt the layer structure. The broad peak at a spacing of 15.9 Å resembles that found for the parent poly(eicosene sulfone)[21] and may correspond to an amorphous component not annealed from this film.

The thin film of polymer **II** has a SAXS pattern with two orders of sharp peaks corresponding to a layer spacing of 40.7 Å and two further broad peaks corresponding to a spacing of 31.5 and 15.7 Å which are presently not understood; the latter may be a measure of the spacings, *s*, within the layer of backbones, or derive from an amorphous component. The SAXS measurements for polymers **I**, **II**, **III**, and **IV** in comparison to the corresponding X-ray measurements in the bulk polymer are given in Table 4. Though measured at ambient temperatures the spacings in the thin films correspond to values measured in the bulk at higher temperatures. The dimensions may differ slightly as these samples are films. Films of the amorphous polymer **V** did not exhibit any sharp peaks in its diffraction pattern and hence did not have a layer structure.

Two polymer films were measured in grazing incidence and in each case only one in-plane peak was found in the range of $0 < q_x < 2$ Å$^{-1}$, parts of which are shown in Figure 10a. From the half-widths of the peaks, lateral correlation lengths of about four to five next neighbor side groups were calculated. For the copolymer **IV** the normalized intensity of the in-plane Bragg-peak was found to be twice of that of the homopolymer **III**. At this angular position, detector scans around the

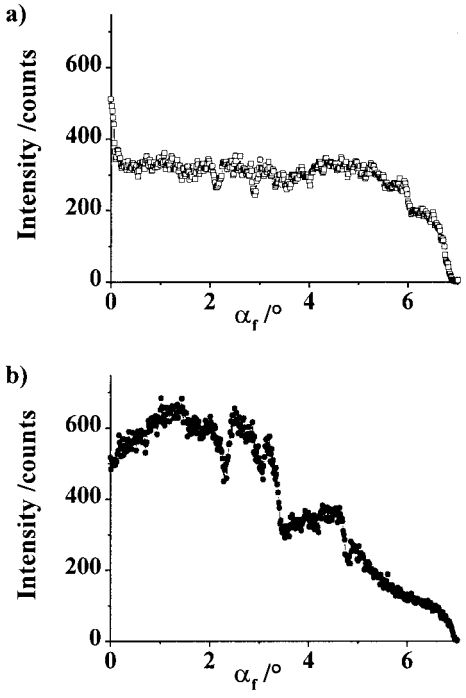


**Figure 11.** "Rod"-scans in the first-order in-plane Bragg-peaks of films of (a) polymer **III** (□) and (b) polymer **IV** (●) with $0 < q_x < 0.9$ Å$^{-1}$.

surface normal were carried out to measure the azimuthal arrangement of the polymer side groups within the films. It was found that there was a modulation in scattering intensity as the angular position, $\omega$, was varied for polymer **IV**, as shown in Figure 10b. Intensity maxima are visible at $\omega = 0$, 90, 240, 270, and 300°, such diffraction features can arise from just two domains in the upper layer of the film. Polymer **III** film shows no preferred orientation in the azimuthal direction as is expected for a fluid smectic phase.

Simultaneously, the crystal truncation rods[60] were recorded. In the case of homopolymer **III** (Figure 11a), the surface peak and, for to higher $\alpha_f$ values, only very slight modulations of the rod were observed. This suggests a vertical domain size which did not much exceed one *d* spacing layer; perhaps each layer is organized independently of its neighbors. The polymer **IV** film did not show the surface peak but gave rise to more intense undulations along $\alpha_f$, Figure 11b, suggesting greater correlation through the layers in this terpolymer film. This suggests that it is a crystalline smectic B phases rather than a hexatic B phase.[61]

**Optical Studies on Films by Circular Dichroism.** We readily found circular dichroism in the annealed films of polymers **I** and **II** when they were inspected at an angle of 45° to the normal, all but negligible signals from the virgin spun films when inspected in the same manner (Figure 12), and no signals at all from their solutions, as the polymers were of course not optically active. The effects from the polysulfone films were within a magnitude of each other, and were generally positive (presumably random) in three or four regions of $\lambda$. The main signal in each CD spectrum of the homopolymers was at about 280 nm, a wavelength that in parts a and b of Figure 4 displayed the largest linear dichroism that we associated with H aggregates. There are also less intense signals at 320 and 370 nm for polymers **I** and **III** there being only a trace of the 320 nm feature in the signal from polymer **III**. Features at the latter wavelengths are not seen in the UV spectra of Figure 4 and may be the only evidence for J aggregates. The side-chain structure of polymer **III** may discourage their formation, and instead favor H aggregates (see Scheme 2).

As polymer **II** showed much less significant CD signals between 220 and 400 nm (and only a small change in the position of the UV absorption maximum on annealing), the CD signal from that polymer correlates with little aggregation of the chromophore. For the cyanobiphenyl homopolymer, the largest CD signal is at 265 nm, even more blue shifted than the maximum of the dichroism (270 nm), which may be consistent with chiral supramolecular structures being higher aggregates. The CD signal from polymer **III** is similarly prominent when measured at a 45° angle, having a major feature at 270 nm, but the signals from the terpolymers are less intense in that geometry. The signals from the homopolymer are bimodal having features at about 270 and 320 nm, but the more isolated chromophores give broad bands centered on 290 nm. Even the amorphous polymer **V** shows a minor effect.

Several structural effects may introduce chirality to this system. First, the cyanobiphenyl rings are nonplanar, the angle of twist being ~40°,[55,56] so the simple biphenyl unit itself is chiral, second, pairs[55] of or higher numbers of cyanobiphenyl groups may be chiral, third, aggregates may be chiral like the pinwheel structures invoked by Whitten[37] or in herringbone patterns,[20,36,51] and finally, there are helices present in the backbone, though these are remote from the chromophores.[8,13] The architecture of the aggregates may generate a chiral assembly, to cause the interactions of the transition moments to change the coupling oscillation strength, as in the exciton−chirality Model.[32,33] When we turn to polymer **III** we find a stronger CD effect after annealing (Figure 12c). Again the maximum is blue-shifted (257 nm) compared to 275 nm for the maximum of the dichroism and 285 nm for the $\lambda_{max}$ of the monomer in hexane. A pair of residues may have a chiral center, or a pinwheel type of structure might form from three or four of them. A graduation from strong CD signals for the biphenyl homopolymers to smaller intensity for the terpolymers and finally no signal for the amorphous polymer confirms the assumption of induced chirality by aggregation, but the structure of the aggregation is elusive.

## Conclusions

When annealed below the clearing temperature, spin-coated films of poly(olefin sulfone)s with one or two cyanobiphenyl side groups per residue developed liquid crystallinity, and the optical and X-ray diffraction properties were considerably modified, so there was no suggestion of an amorphous component. The annealing process caused a spontaneous self-assembly to form a new type of smectic structure, in which the rodlike side groups are homeotropically aligned and aggregated, and helices form in the backbones as electrostatic effects between the sulfone dipoles become effective, and then their helices attract each other to become planar aligned over the film. Polymers **I** and **III** fit the model of Scheme 2, in which the structure-determining features are the cross-sectional area of the aromatic mesogens and the pitch of the backbone helix. The clearing temperature rose and interlayer spacing *d* fell as the number of mesogens per residue was changed from 1

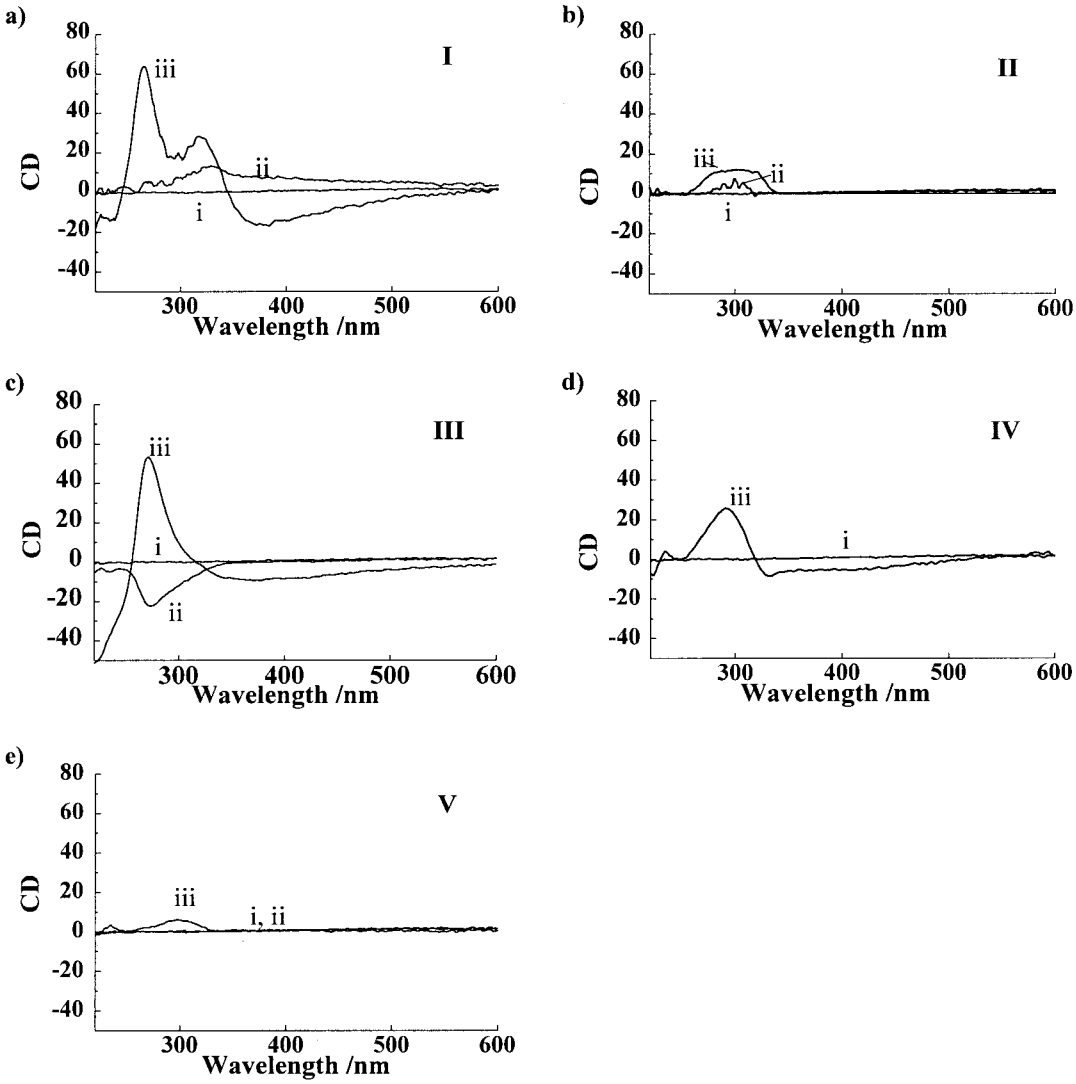


**Figure 12.** CD spectra of the polymers **I** (a), **II** (b), **III** (c), **IV** (d), and **V** (e) as virgin film (i), annealed film NP (ii) and annealed film ZP (iii).

to 2. A glass transition temperature at about 15 °C was associated with the spacers. Both the initial and the annealed films were optically isotropic when examined at a normal direction, but the annealed films showed also a significant dichroism of the $\pi-\pi^*$ transition on measuring the sample in a tilted orientation, the $\lambda_{max}$ shift indicating H aggregates. The spontaneous orientation of the side groups led to a significant decrease of the $\pi-\pi^*$ absorbance of the biphenyl moieties when measured in the normal direction and resulted in spectroscopic degrees of order as high as 0.63−0.50 for the smectic homopolymers bearing two and one side chain mesogens respectively per residue. Enhancing *s* reduces the order possible in the side chains. The ordered films were optically clear and did not scatter light, indicating the formation of a homeotropically aligned monodomain of the side groups of the liquid crystalline polymers. There was not just a thermotropic self-organization to form domains, but X-ray reflection and SAXS indicated the film has a layered structure of the backbones parallel to the interfaces which went through the whole film. For the crystalline polymer **IV** there were probably only two domains in the surface layer, the spacing of which corresponded to the penetration depth.

Annealing spun films of polymers **II** and **IV** by cooling also yielded layered structures, together with some amorphous content, with only polymer **IV** having a fluid smectic A phase, with in a small temperature range. At room temperature the crystalline B phases again extended over the plane of the substrate, but the diluted chromophores were only partly aligned normal to the plane. Helicity and polarity of the backbones created these layers, as in poly(eicosenesulfone), but the small fraction of aromatic units suppressed or limited the formation of a fluid smectic phase and promoted crystallization.

Accompanying the molecular self-association of the biphenyl moieties in **I** and **III**, $\pi-\pi$ interactions caused the formation of dimers or clusters of chromophores. This was not seen in the liquid crystalline or amorphous polymers in which only a few residues bore such groups, but there was a small effect when as in polymer **IV**, the mesogenic units came in pairs, perhaps when larger aggregates formed. An exclusive content of mesogens in the side chain and the enforced organization in the liquid crystalline poly(olefin sulfone) homopolymers favored such packing. The aggregates were the most homeotropically aligned structures in **I** and **III**; they were characterized by a blue shift in absorption, a red

shift in fluorescence, and an induced circular dichroism. The spectral shift is ascribed to exciton interaction between the aromatic side groups in H aggregates,[32,33] the absence of J aggregates perhaps indicating a $P_1$ type of interdigitation in the partial bilayer (Scheme 2). Moreover, the induced circular dichroism showed that the aggregated side groups of the poly(olefin sulfone)s formed a chiral supramolecular structure. This finding within such planar fluid layers is an extension of recent results concerning aggregated achiral chromophores in phospholipid bilayers[37,62,63] within micelles and spontaneous formation of chirality in the case of J aggregates of achiral cyanine dyes.[42] Cyclic tetramer units ("pinwheel") or herringbone lattices have been discussed[20,37,62−64] as supramolecular structures producing this effect, but in the present case, the helical sense of the backbones may feature, though they are rather remote. So the spectral properties of the chromophores are strongly affected by their mode of orientation and aggregation by the ordered microenvironment in the two-dimensional layers of these polymers.

The structure−property relationships suggests that these orientation and aggregation phenomena in thin films were driven by the liquid crystallinity and the segregation tendency of the two components, the polar backbone and aromatic side groups of these polymers. These effects were missing from the amorphous poly(olefin sulfone), polymer **V**, and the smectic poly(methacrylate), polymer **VI**, with identical cyanobiphenyl side groups. The comparison of the homopolymers **I** and **III** with poly(eicosene/biphenyl) copolymers **II** and **IV** shows the requirement for a full complement of the stiff, aromatic side groups in the side chain orientation process. In contrast to these poly(olefin sulfone)s other combined main and side chain liquid crystalline polymers with comparable side chain mesogenic groups tend to have alignment of the rodlike side groups parallel to the polyglutamate[34] or aromatic[65] backbones. Polar effects within the polysulfone backbones cause helices to form, polar effects between the backbones causes them to form planar layers, and the aromaticity of the side chains cause a homeotropic self-assembly. For this supramolecular structure we introduce the term homeoplanar smectic.

**Acknowledgment.** We thank the EPSRC and the DRA for support to R.W.D., the DFG for support to J.H. (SFB337), and the DAAD and the British Council for travel funds. We thank Dr. R. Ruhmann of the Institute for Applied Chemistry, Berlin-Adlershof, Germany, for the sample of polymer **VI**, S. Pade of the University of Potsdam for providing the fluorescence measurements, J. Wagner of the Humboldt University Berlin for the CD measurements, and also H. Rhan and T. Brückel of Hasylab, DESY, Hamburg, Germany, for their assistance with the synchrotron experiments, Dr. J. M. Seddon of Imperial College, London, for help with the bulk X-ray studies, and Dr G.S. Attard of Southampton University for useful discussions. Financial support for the in-plane measurements came from the German Bundesministerium of Education and Research under 055IPAAI8 and the DFG (Grants Stu 164/3-1 and Pi 217/4-3) and is gratefully acknowledged.

## References and Notes

(1) Fawcett, A. H. *Encyclopedia of Polmer Science and Engineering,* 2nd ed.; Kroschwitz, J. I., Ed.; J. W. Wiley and Sons: New York, 1989, *10*, 408.
(2) Braun, D.; Herr, R.-P.; Arnold, N. *Macromol. Chem. Rapid Comm.* **1987**, *8*, 359.
(3) Arnold, N.; Braun, D.; Hirschmann, H.; Wendorff, J. H. *Macromol. Chem. Rapid Commun.* **1988**, *9*, 331.
(4) Fawcett, A. H.; Szeto, D. Y. S. *Polymer Commun.* **1991**, *32*, 77.
(5) Braun, D.; Arnold, N.; Leibmann, A.; Schmidkte, I. *Macromol. Chem.* **1993**, *194*, 2687.
(6) Dass, N. N.; Date, R. W.; Fawcett, A. H.; McLaughlin, J. D.; Sosanwo, O. A. *Macromolecules* **1993**, *26*, 4192.
(7) Dass, N. N.; Date, R. W.; Fawcett, A. H.; Lapienis, G. *Polymer Prepr. (Am. Chem. Soc., Div. Polym. Chem.)* **1994**, *35* (1), 156.
(8) Cole, R. H.; Winsor, P.; Fawcett, A. H.; Fee, S. *Macromolecules* **1987**, *20*, 157.
(9) Heatley, F.; Fawcett, A. H.; Ivin, K. J.; Stewart, C. D.; Watt, P. *Macromolecules* **1977**, *10*, 765.
(10) Fawcett, A. H.; Fee, S. *Macromolecules* **1982**, *15*, 933.
(11) Mansfield, M. *Macromolecules* **1982**, *15*, 1587.
(12) Matsuo, K.; Mansfield, M. L.; Stockmayer, W. H. *Macromolecules* **1982**, *15*, 935.
(13) Mashimo, S.; Winsor, P.; Cole, R. H.; Matsuo, K.; Stockmayer, W. H. *Macromolecules* **1986**, *19*, 682.
(14) Ruben, G. C.; Stockmayer, W. H. *Proc. Natl. Acad. Sci. U.S.A.* **1992**, *89*, 11645.
(15) Fawcett, A. H.; Fee, S.; Waring, L. *Polymer* **1983**, *24*, 1571.
(16) Bates, T. W.; Ivin, K. J.; Williams, G. *Trans. Faraday Soc.* **1967**, *63*, 1976.
(17) Stockmayer, W. H.; Jones, A. A.; Treadwell, T. L. *Macromolecules* **1977**, *10*, 762.
(18) Baysal, B.; Erbil, C.; Morganelli, P. L.; Stockmayer, W. H. *Turk. J. Chem.* **1997**, *21*, 239.
(19) Watanabe, J.; Takashima, Y. *Macromolecules* **1991**, *24*, 3423.
(20) Kang, C. S.; Winkelhahn, H. J.; Schulze, M.; Neher, D.; Wegner, G. *Chem. Mater.* **1994**, *6*, 2159.
(21) Date, R. W.; Fawcett, A. H. Unpublished work.
(22) Zentel, R., *Liquid Crystals*; Stegemeyer, H., Ed.; Topics in Physical Chemistry 3; Spinger: New York, 1994.
(23) Tsukruk, V. V. *Prog. Polym. Sci.* **1997**, *22*, 247.
(24) Yitzchaik, S.; Marks, T. J. *Acc. Chem. Res.* **1996**, *29*, 197.
(25) Vyov, V.; Decher, G.; Sukhorukov, G. *Macromolecules* **1993**, *26*, 5396.
(26) Attard, G. S.; Williams, G.; Fawcett, A. H. *Polymer* **1987**, *31*, 928.
(27) Nazemi, A.; Kellar, E. J. C.; Williams, G.; Karasz, F.; Hill, J. S.; Lacey, D.; Gray, G. W. *Liq. Cryst.* **1991**, *9*, 307.
(28) Findlay, R. B.; Windle, A. H. *Mol. Cryst. Liq. Cryst.* **1991**, *206*, 55.
(29) Uto, S.; Ohtsuki, H.; Ozaki, M.; Yoshino, K. *Jpn. J. Appl. Phys. Part 1* **1996**, *35* (9b), 5050.
(30) Davidov, D.; Tarabia, M.; Cohen, G.; Keller, P. *Isr. J. Chem.*, **1995**, *35* (1), 3.
(31) Chen, H. J.; Law, K.; Perlstein, J.; Whitten, D. G. *J. Am. Chem. Soc.* **1995**, *117*, 7257.
(32) Kasha, M. *Radiat. Res.* **1963**, *55*, 20.
(33) Kasha, M. In *Spectroscopy of Excited States*; Bartolo, B. D., Ed.; Plenum Press: New York, 1976.
(34) Stumpe, J.; Fischer, T.; Menzel, H., *Macromolecules,* **1996**, *29*, 2831.
(35) Shimomura, M.; Ando, R.; Kunitake, T. *Ber. Bunsen-Ges. Phys. Chem.* **1983**, *87*, 1134.
(36) Kunitake, T. *Angew. Chem., Int. Ed. Engl.* **1992**, *31*, 709.
(37) Whitten, D. G. *Acc. Chem. Res.* **1993**, *26*, 502.
(38) Creed, D.; Griffin, A. C.; Gross, J. R. D.; Hoyle, C. E.; Venkataram, K. *Mol. Cryst. Liq. Cryst.* **1988**, *155*, 57.
(39) Sapich, B.; Haferkorn, J.; Läsker, L.; Stumpe, J. *J. Inf. Rec.* **1996**, *23*, 103.
(40) Haferkorn, J.; Sapich, B.; Geue, T.; Stumpe, J.; Date, R. W.; Fawcett, A. H., *Proc. Liq. Cryst. Conf. Freiburg* **1996**, *26*, 25.
(41) Haferkorn, J.; Stumpe, J., *J. Inf. Recording*, **1996**, *23*, 107.
(42) De Rossi, U.; Dähne, S.; Meskers, S. C. J.; Dekkers, H. P. J. M. *Angew. Chem., Int. Ed. Engl.* **1996**, *35*, 760.
(43) Lehn, J. M. *Supramolecular Chemistry*; VCH: Cambridge, England, 1995.
(44) Kelker, H.; Hatz, R.; Wirzing, G. *Z. Anal. Chem.* **1973**, *267*, 161.
(45) Als-Nielsen, J.; Möhwald, H. In *Handbook of Synchrotron Radiation*; Ebashi, S., Koch, M., Rubinstein, E., Ed.; Elsevier, Oxford, England, 1991; Vol. 4.
(46) Sinha, S. K.; Sirota, E. B.; Garoff, S.; Stanley, H. B. *Phys. Rev. B* **1988**, *38*, 2297.
(47) Merle, H. J.; Metzger, H.; Pietsch, U. *Phys. Scr.* **1992**, *T45*, 253.

(48) Metzger, T. H.; Luidl, C.; Pietsch, U.; Vierl, U. *Nucl. Instrum. Methods,* **1994**, *A350,* 398.
(49) Geue, T.; Pietsch, U.; Stumpe, J. *Thin Solid Films* **1996**, *285,* 228.
(50) Paschke, K.; Geue, T.; Barberka, T.; Bolm, A.; Pietsch, U.; Roesch, M.; Batke, E.; Oshinowo, J.; Forchel, A. *Appl. Phys. Lett.*. **1997**, *70,* 1031.
(51) Robinson, I. K.; Tweet, D. J. *Rep. Prog. Phys.* **1992**, *55,* 599.
(52) Watanabe, J.; Tominaga, T. *Macromolecules* **1993**, *26,* 4032.
(53) Leadbetter, A. J. *Thermotropic Liquid Crystals*; Gray, G. W., Ed.; J. W. Wiley: Chichester, England, 1987.
(54) Platé, N. A.; Shibaev, V. P. *J. Polym. Sci.: Macromol. Rev.* **1974**, *8,* 117.
(55) Leadbetter, A. J.; Frost, J. C.; Gaughan, J. P.; Gray, G. W.; Mosley, A. *J. Phys.* **1979**, *40,* 375.
(56) Brock, C. P.; Kuo, M. S.; Levy, H. A. *Acta Crystallogr.* **1978**, *B34,* 981.
(57) Counsell, C. J. R.; Emsley, J. W.; Luckhurst, G. R.; Sachdev, H. S. *Mol. Phys.* **1988**, *63,* 33.
(58) Zeiss miscroscope spectrometer.
(59) Flory, P. J. *Statistical Mechanics of Chain Molecules*; Interscience: New York, 1969.
(60) Gau, T. S.; Chang, S. L. *Acta Crystallogr.* **1995**, *A51,* 920.
(61) Gane, P. A. C.; Leadbetter, A. J.; Wrighton, P. G. *Mol. Cryst. Liq. Cryst.* **1981**, *66,* 247.
(62) Song, X. D.; Geiger, C.; Leinhos, U.; Perlstein, J.; Whitten, D. G. *J. Am. Chem. Soc.* **1994**, *116,* 10340.
(63) Song, X. D.; Perlstein, J.; Whitten, D. G. *J. Am. Chem. Soc.* **1995**, *117,* 7816.
(64) Chen, J. T.; Thomas, E. L.; Ober, C. K.; Mao, G. P. *Science* **1996**, *273,* 343.
(65) Hohmuth, A.; Weissflogg, W. *Proc. Liq. Crys. Conf., Freiburg* **1996**, *25,* 48.

MA971827P